

## **1. INTRODUCTION**

Since 1963, all United States nuclear tests have been conducted underground. A consequence of this testing has been the deposition of large amounts of radioactive material in the subsurface, sometimes in direct contact with groundwater. The majority of this testing occurred on the Nevada Test Site (NTS), but a limited number of experiments were conducted in other locations. One of these locations, Amchitka Island, Alaska is the subject of this report.

Three underground nuclear tests were conducted on Amchitka Island. Long Shot was an 80-kiloton-yield test conducted at a depth of 700 meters (m) on October 29, 1965 (DOE, 2000). Milrow had an announced yield of about 1,000 kilotons, and was detonated at a depth of 1,220 m on October 2, 1969. Cannikin had an announced yield less than 5,000 kilotons, and was conducted at a depth of 1,790 m on November 6, 1971.

Evaluation of groundwater contamination caused by nuclear testing on Amchitka is being conducted by the U.S. Department of Energy (DOE), in consultation with the State of Alaska Department of Environmental Conservation and the Aleutian/Pribilof Islands Association, Inc.

### **1.1 Purpose and Organization**

The purpose of this work is to provide a portion of the information needed to conduct a human-health risk assessment of the potential hazard posed by the three underground nuclear tests on Amchitka Island. Specifically, the focus of this work is the subsurface transport portion, including the release of radionuclides from the underground cavities and their movement through the groundwater system to the point where they seep out of the ocean floor and into the marine environment. This requires a conceptual model of groundwater flow on the island using geologic, hydrologic, and chemical information, a numerical model for groundwater flow, a conceptual model of contaminant release and transport properties from the nuclear test cavities, and a numerical model for contaminant transport.

Needed for the risk assessment are estimates of the quantity of radionuclides (in terms of mass flux) from the underground tests on Amchitka that could discharge to the ocean, the time of possible discharge, and the location in terms of distance from shoreline. The radionuclide data presented here are all reported in terms of normalized masses to avoid presenting classified information. As only linear processes are modeled, the results can be readily scaled by the true classified masses for use in the risk assessment. The modeling timeframe for the risk assessment was set at 1,000 years, though some calculations are extended to 2,000 years.

This first section of the report endeavors to orient the reader with the environment of Amchitka and the specifics of the underground nuclear tests. Of prime importance are the geologic and hydrologic conditions of the subsurface. A conceptual model for groundwater flow beneath the island is then developed and paired with an appropriate numerical modeling approach in section 2. The parameters needed for the model, supporting data for them, and data uncertainties are discussed at length. The calibration of the three flow models (one for each test) is then presented. At this point the conceptual radionuclide transport model is introduced and its numerical approach described in section 3. Again, the transport parameters and their supporting data and uncertainties are the focus.

With all of the processes and parameters in place, the first major modeling phase can be discussed in section 4. In this phase, a parametric uncertainty analysis is performed to determine the sensitivity of the transport modeling results to the uncertainties present in the parameters. This analysis is motivated by the recognition of substantial uncertainty in the subsurface conditions on the island and the need to incorporate that uncertainty into the modeling. The conclusion of the first phase determines the parameters to hold as uncertain through the main flow and transport modeling. This second, main phase of modeling is presented in section 5, with the contaminant breakthrough behavior of each test site addressed. This is followed by a sensitivity analysis in section 6, regarding the importance of additional processes that could not be supported in the main modeling effort due to lack of data. Finally, the results for the individual sites are compared, the sensitivities discussed, and final conclusions presented in section 7.

## 1.2 Previous Work

Amchitka Island was chosen as a Supplemental Test Site (STS) for underground testing of nuclear explosives, a designation which was preceded by thorough characterization of the island geology. Investigations in direct support of Milrow and Cannikin added site-specific data to the island-wide picture. Much of the work supporting these activities is listed in a bibliography of reports by U.S. Geological Survey (USGS) personnel on the geology and hydrology of Amchitka Island (Ohl, 1973). Long Shot actually preceded the STS selection and some of its important references are not in USGS reports. Important references for the island as a whole, and the individual tests, are listed below (Table 1.1). Detailed reports describing geologic and hydrologic data are not included here, but are referenced in appropriate later sections.

Table 1.1. Selected references for island-wide investigations and individual tests.

Investigation	Scope
Selected Island-wide Investigations	
Ohl, 1973	Bibliography of USGS reports on Amchitka
U.S. AEC, 1967	Site-selection report describing geology and hydrology
Carr <i>et al.</i> , 1969	Geologic reconnaissance of the island
Carr and Quinlivan, 1969	Updated geologic information
von Huene <i>et al.</i> , 1971	Geophysical study of Amchitka
Bath <i>et al.</i> , 1971	Gravity survey of Amchitka
Anderson, 1971	Tectonic setting of Amchitka
Carr <i>et al.</i> , 1971	Summary paper of stratigraphy, structure, etc.
Gates <i>et al.</i> , 1954	Aleutian geology with reference to Amchitka
Beetem <i>et al.</i> , 1971	Chemical analyses of water samples
Gard, Jr., 1972	Chemical analyses of rock samples
Lee, 1969a, b, c, d	Physical rock properties
Bath <i>et al.</i> , 1972	Aeromagnetic survey of Amchitka
Merritt and Fuller, 1977	Summary papers on climate, geology, hydrology and biota
Wheatcraft, 1995	Seawater intrusion model of the island

Table 1.2. Selected references for island-wide investigations and individual tests (continued).

Investigation	Scope
<b>Selected Long Shot Investigations</b>	
Nork <i>et al.</i> , 1965	Groundwater safety analysis
Gard and Hale, 1964	Geology and hydrology
U.S. Army Corps of Engineers and U.S. Geological Survey, 1965	Geology and hydrology, with hydrologic and core data in extensive appendices
<b>Selected Milrow Investigations</b>	
U.S. Geological Survey, 1970	Geologic and hydrologic effects of Milrow
Essington <i>et al.</i> , 1970	Radionuclide transport analysis
<b>Selected Cannikin Investigations</b>	
Lee and Gard, Jr., 1971	Summary of subsurface geology
Gonzalez and Wollitz, 1972	Hydrologic effects of the test
Fenske, 1972a, b	Hydrologic transport of radionuclides
Gonzalez, 1977	Hydraulic effects of the test
Claassen, 1978	Near-cavity processes associated with the test
Merritt, 1973	Summary of physical and biologic effects of the test
U.S. Geological Survey, 1972	Geologic and hydrologic effects of the test
<b>Selected Monitoring Investigations</b>	
U.S. DOE, 1982	Description of long-term hydrologic monitoring program
Castagnola, 1969	Study of tritium anomalies at Long Shot
Essington <i>et al.</i> , 1971	Radionuclide and water-level monitoring data for Long Shot and Milrow

### 1.3 General Description of Amchitka Island

Amchitka is the southernmost island of the Rat Island Group of the Aleutian Island chain extending southwestward from mainland Alaska (Figure 1.1). It is located between longitudes 178°37'E and 179°29'E, and between latitudes 51°21'N and 51°39'N. Amchitka is almost half-way from North America to Asia, and is 2,160 km west-southwest of Anchorage. Amchitka is part of the Aleutian Islands National Wildlife Refuge. It is bounded on the northeast by the Bering Sea and on the southwest by the Pacific Ocean.

The island is about 65 km long and varies between 2 and 7 km wide (Merritt, 1977). Elevation varies from sea level at the few beaches to 354 m above mean sea level (AMSL). Most of the shoreline is rugged and characterized by cliffs up to 30 m high. Topographically, the island can be divided into three areas (Figure 1.2). The eastern half is a lowland plateau characterized by gently rolling topography below 100 m elevation and many shallow ponds. Low, but abundant, vegetation covers the landscape in this area. The central mountain segment west of Chitka Point is where the maximum elevation of 354 m is reached. This region has fewer lakes, more integrated drainage, and sparse vegetation. The westernmost end of the island is a high plateau at an elevation of about 240 m,

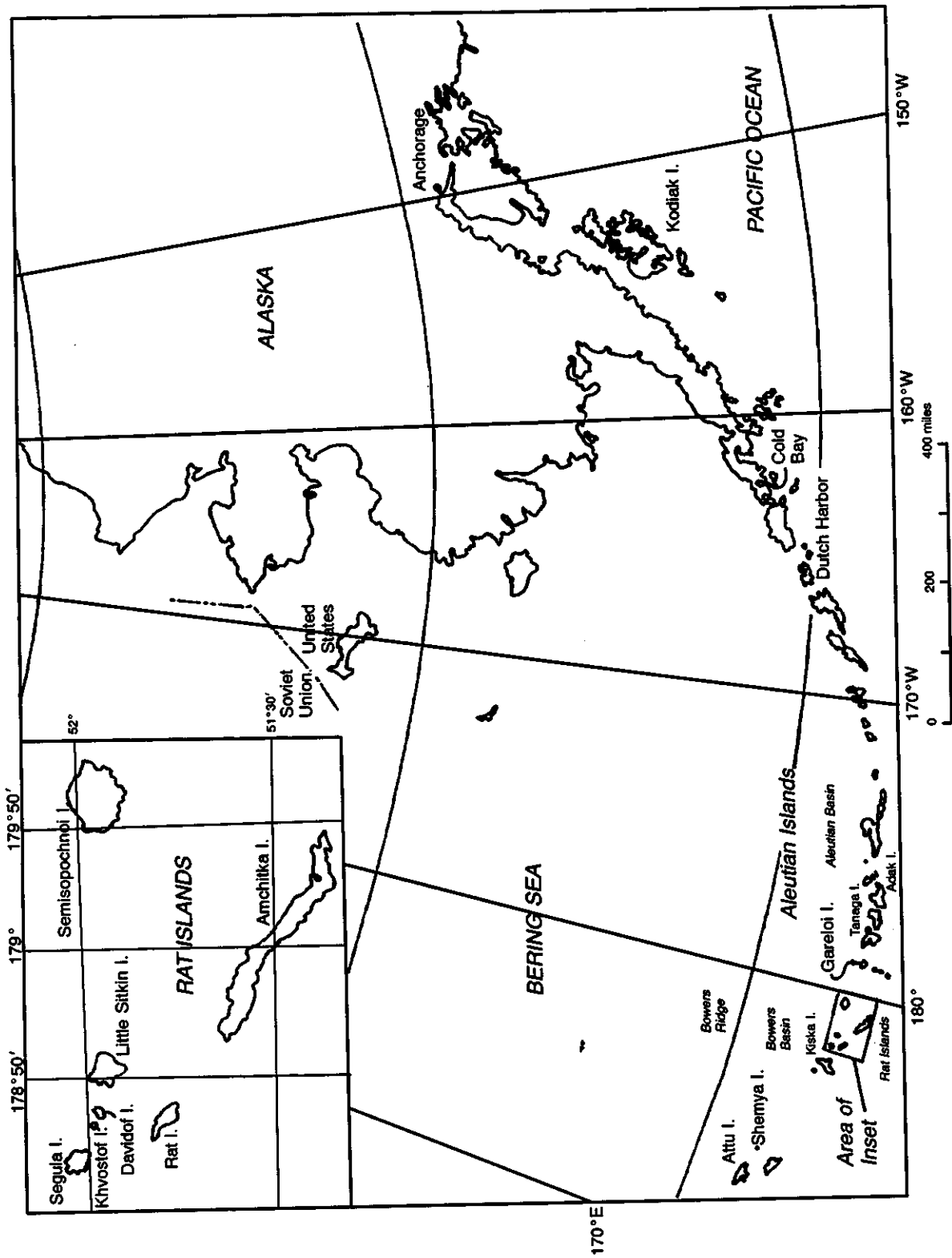


Figure 1.1. Location map showing Amchitka Island in the Aleutian Island chain.

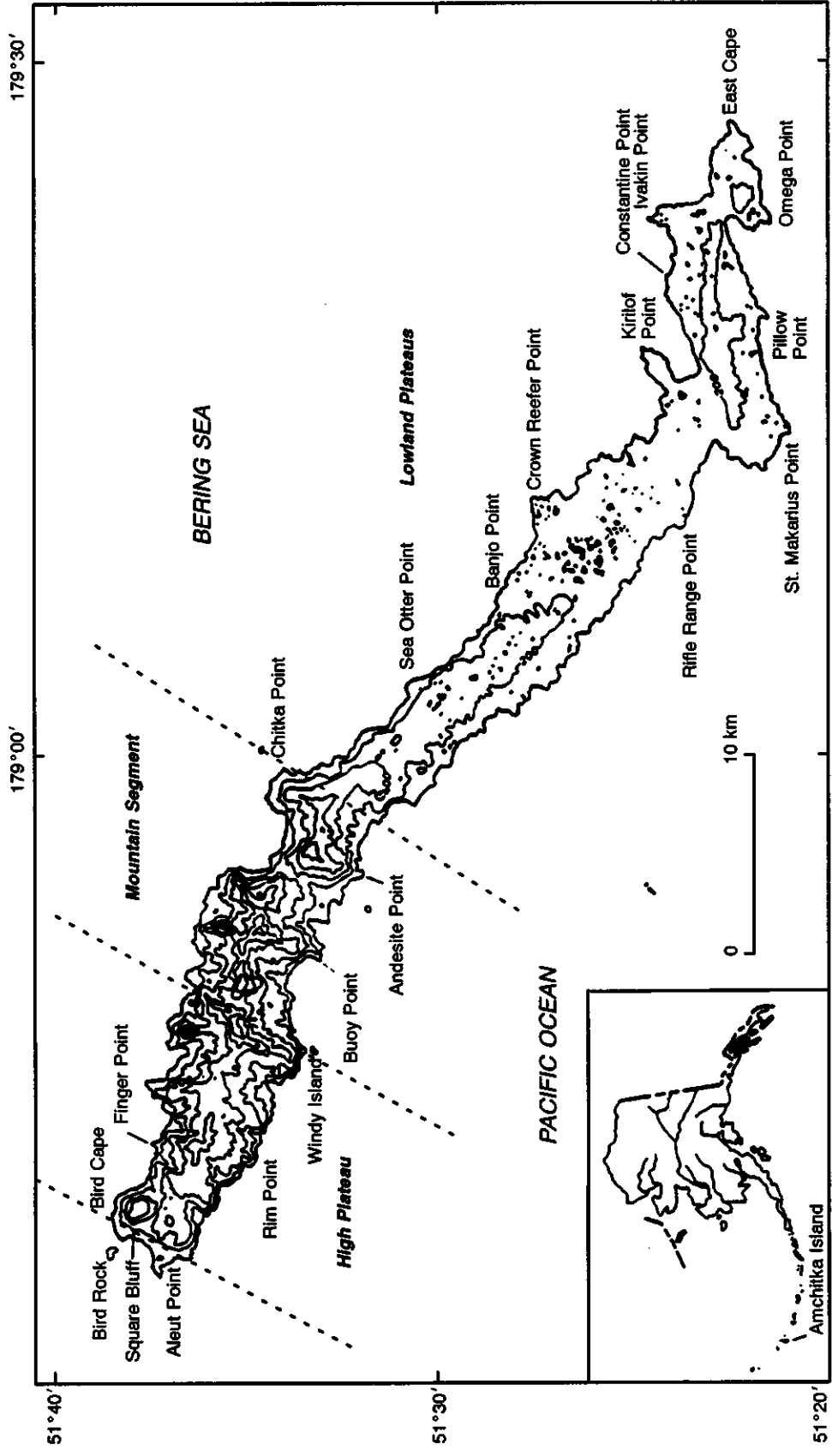


Figure 1.2. Locations and topography of Amchitka Island (from Gonzalez, 1977). Topographic contours are in feet AMSL, contour interval 200 feet (one foot = 0.3048 m).

windswept and barren. All of the underground tests, and the majority of detailed investigations, occurred in the Lowland Plateau region.

Amchitka has a maritime climate, being foggy and windswept much of the time. Partial to complete cloud cover occurs 98 percent of the time (Gonzalez, 1977). Aleutian weather results almost entirely from large-scale pressure systems moving along the North Pacific storm track. Climate data are available from the Desert Research Institute's (DRI) Western Regional Climate Center in Reno, Nevada, but reflect only a few years of record in 1949-1950, 1979-1980, and 1988-1993. The moderating influence of the surrounding ocean is evident in the relatively small range in average temperatures: the highest monthly average maximum temperature is 10.8°C and occurs in August, while the lowest monthly average minimum is -2.2°C and occurs in February. Average annual precipitation is 94 cm, with lowest amounts in the spring months and greatest precipitation in the late summer (Figure 1.3). Summer is also a time of extensive fog development, with summer fog often persisting for days at a time (Armstrong, 1977). Average snowfall totals 129 cm per year.

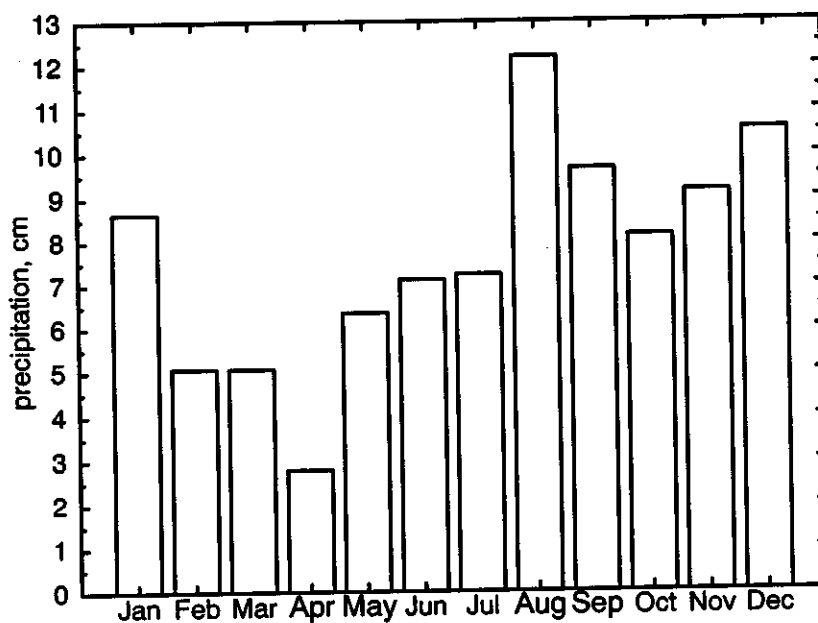


Figure 1.3. Average total monthly precipitation at Amchitka Island (from DRI's Western Regional Climate Center).

#### 1.4 Description of the Underground Nuclear Test Sites

The three tests are described below, and throughout this report, in geographic order from the southeast to the northwest. Milrow is first, followed by Long Shot and Cannikin.

##### 1.4.1 Milrow

The Milrow test was a "calibration shot," designed to produce a database for extrapolation and prediction of the impact of larger nuclear tests, specifically, as to whether it would be safe to conduct the Cannikin test (Merritt, 1973). The site location is also known as "site B" in much of the earlier literature regarding Amchitka site selection (Figure 1.4). Milrow was fired on October 2, 1969, at

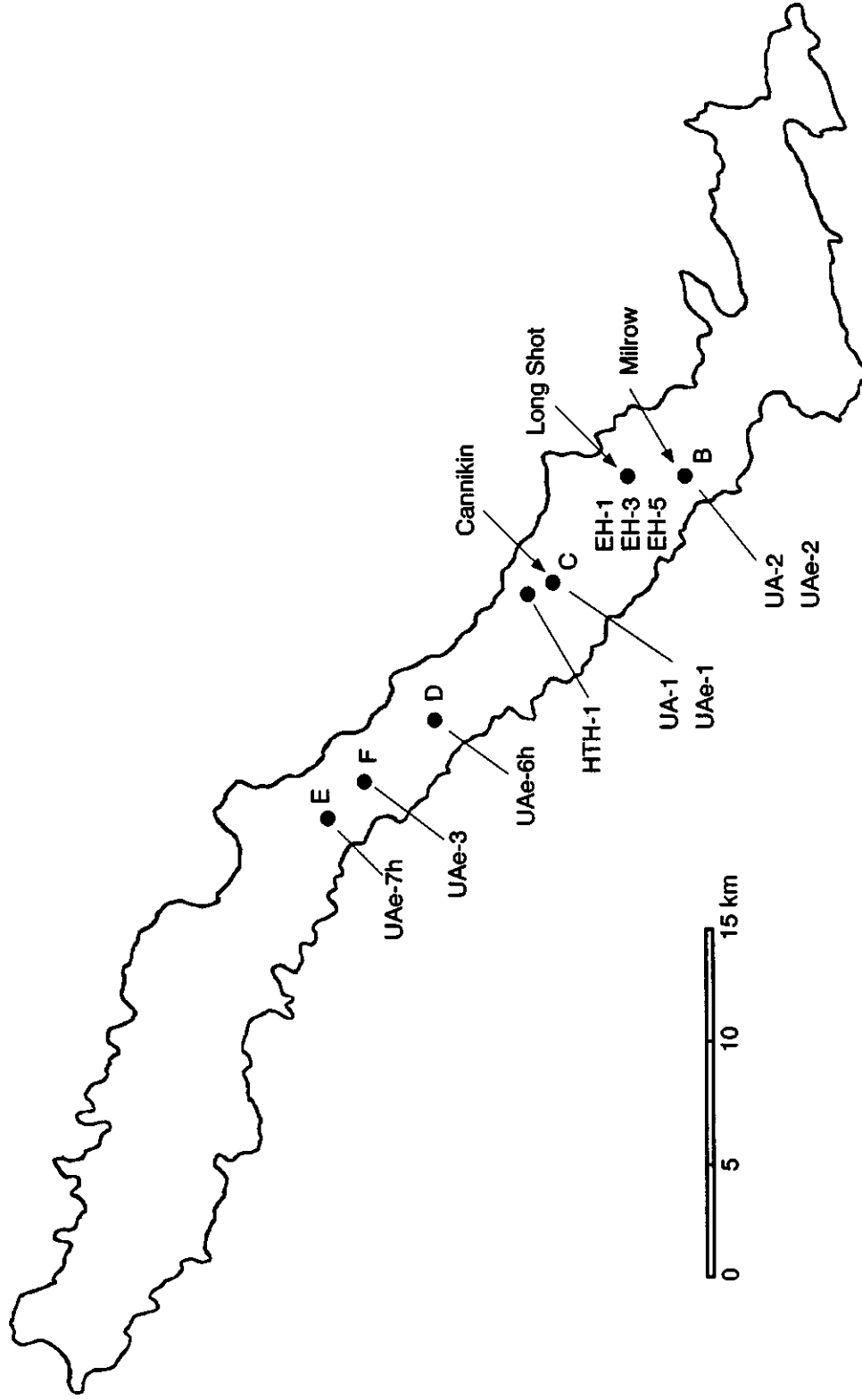


Figure 1.4. Location map showing the exploratory locations for the Supplemental Test Site program (letters B through F) and boreholes discussed in the text.

a depth of 1,218 m below land surface, with an announced yield of about one megaton (U.S. DOE, 1994).

Milrow was the only test detonated on the Pacific Ocean side of the island, at UTM coordinates N 5,698,251.49 m, E 651,750.61 m, zone 60 (USGS, 1970). The island half-width is taken as 2,062 m on the transect from the groundwater divide through Milrow to the coast. Milrow itself is 765 m from the divide (Figure 1.5). The collar elevation of the emplacement hole was 39.8 m. Using the rough, generic relationships between yield and cavity size, and yield and depth of burial, and cancelling out yield (Glasstone and Dolan, 1977) leads to an estimated cavity radius of 106 m. The collapse of material into the cavity void led to a surface collapse feature (Figure 1.6), and given the uncertainty regarding the degree of fracturing between the rubble-filled chimney (generally only four to six times the cavity radius; Glasstone and Dolan, 1977), the spall zone, and the surface collapse, the entire length from the cavity to land surface is considered disrupted in the model.

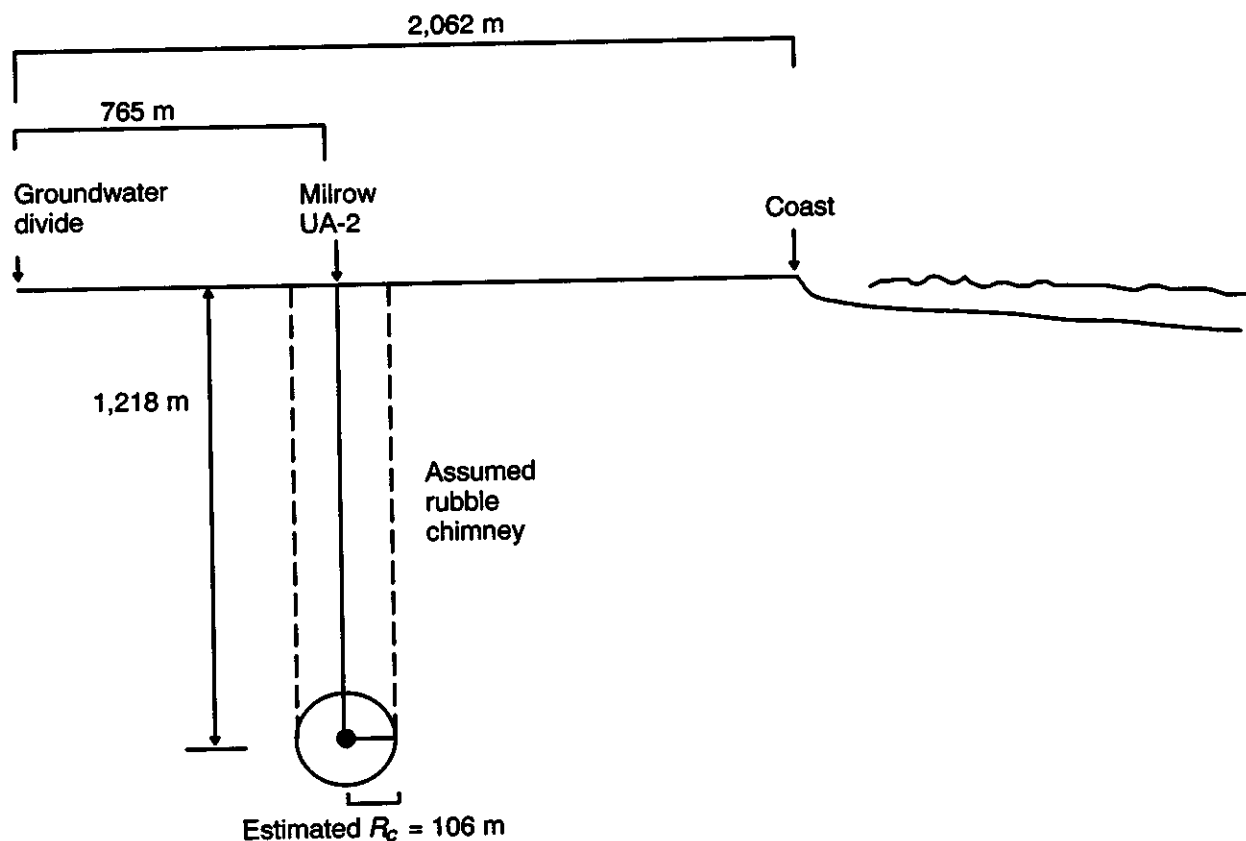


Figure 1.5 Schematic cross section of the Milrow test and relevant features, scale approximate.

### 1.4.2 Long Shot

The Long Shot test was part of the U.S. Department of Defense Vela Uniform program investigating the seismic detection of nuclear tests; specifically, determining location accuracy and seismic wave travel times near island arcs and oceanic trenches. Long Shot was conducted on October 29, 1965, and had an announced yield of 80 kt (U.S. DOE, 2000).

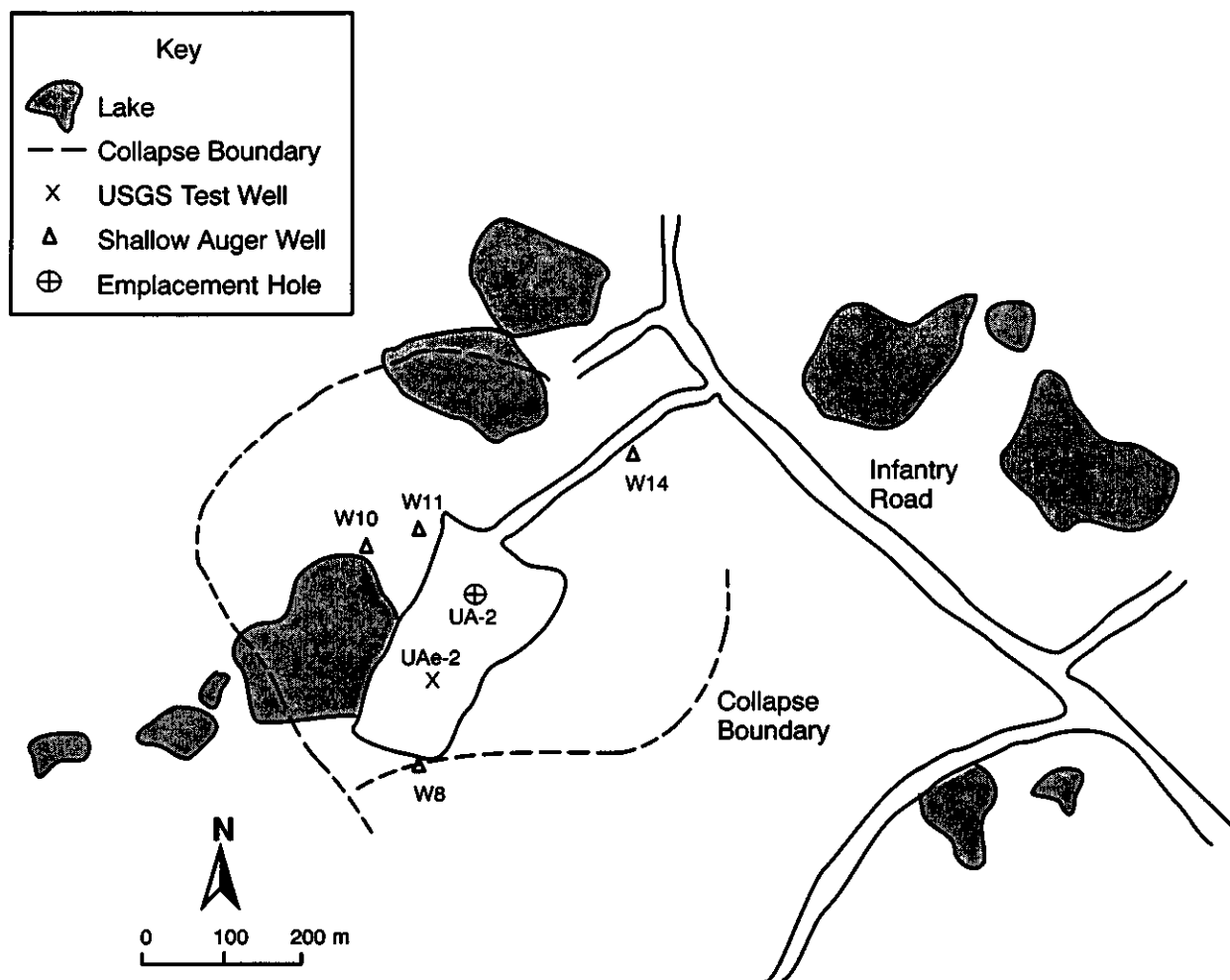


Figure 1.6. Location map showing wells and boreholes in the immediate vicinity of Milrow. The surface collapse area resulting from the test is also shown. Modified from Essington *et al.* 1971.

The ground zero location was at approximate UTM coordinates N 5,700,585 m, E 651,652 m, zone 60. This is located on the Bering Sea-side of the island, approximately 599 m from the groundwater divide (Figure 1.7). The island half-width is taken as 2,224 m on the transect from the divide through Long Shot and to the coast. The land elevation is 42 m. The depth of the device was 701 m below land surface. The cavity radius is variously estimated as 63 m (Nork *et al.*, 1965) and 65 m (McKeown *et al.*, 1967). For consistency with the cavity estimates of the other tests, a value of 61 m is used here, from a calculation based on the depth of burial (Glasstone and Dolan, 1977). Though the chimney height is likely on the order of 300 m (five times the cavity radius; Glasstone and Dolan, 1977), the entire zone above the cavity to land surface is considered disrupted in the model.

There is no surface collapse at the Long Shot site. Spalling (fracturing caused by the pressure wave encountering the free-air surface) was predicted to occur between depths of 30 and 150 m (U.S. Atomic Energy Commission (AEC), 1967). Tritium and krypton were found in surface water ponds

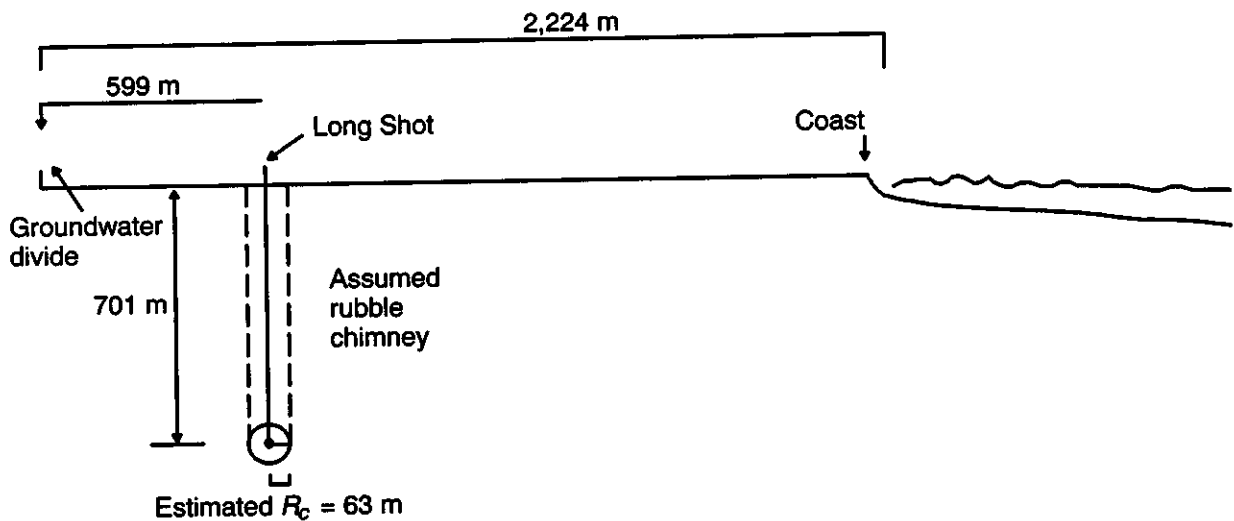


Figure 1.7. Schematic cross section of the Long Shot test and pertinent features, scale approximate.

and mud pits following the test, which led to investigations in several wells. The layout of the site is shown in Figure 1.8. Maximum concentrations occurred in samples collected at depths between 61 and 91 m, and decreased with distance from ground zero. The source was believed to be gases that migrated to the top of the Long Shot chimney in early time. As the chimney filled with water, it is postulated that the gases were pushed upward through stemming material, out into the spill zone, and then dissolved in groundwater (Castagnola, 1969). This spreading upward of the gaseous radionuclide source has not been included in the model. The effect would be to spread the mass through a greater volume, reducing the point mass flux and resultant concentrations. In addition, as there is a strong component of downward vertical flow, the path length for any particles placed higher in the chimney could be longer than that obtained by starting them in the cavity.

#### 1.4.3 Cannikin

The Cannikin test was designed to proof-test the Spartan warhead for use in an anti-ballistic missile system (Merritt, 1973). It was detonated on November 6, 1971, and had an announced yield of less than five megatons (U.S. DOE, 1994).

The emplacement well for Cannikin was UA-1 and is located at UTM coordinates N 5,704,185.92 m, E 646,321.59 m, zone 60. The general location is also known as Site "C" in many of the STS characterization reports. Cannikin is located on the Bering Sea side of Amchitka Island. The island half-width, from groundwater divide, through Cannikin, and to the Bering Sea, is estimated as 2,328 m, with UC-1 located 811 m from the divide (Figure 1.9). The land elevation at the emplacement hole was 63.3 m, but there is land subsidence as a result of the test. The depth of the device was 1,791.9 m below land surface. The cavity radius used here is based on a generic relationship with depth of burial (Glasstone and Dolan, 1977), and is estimated as 157 m. Claassen

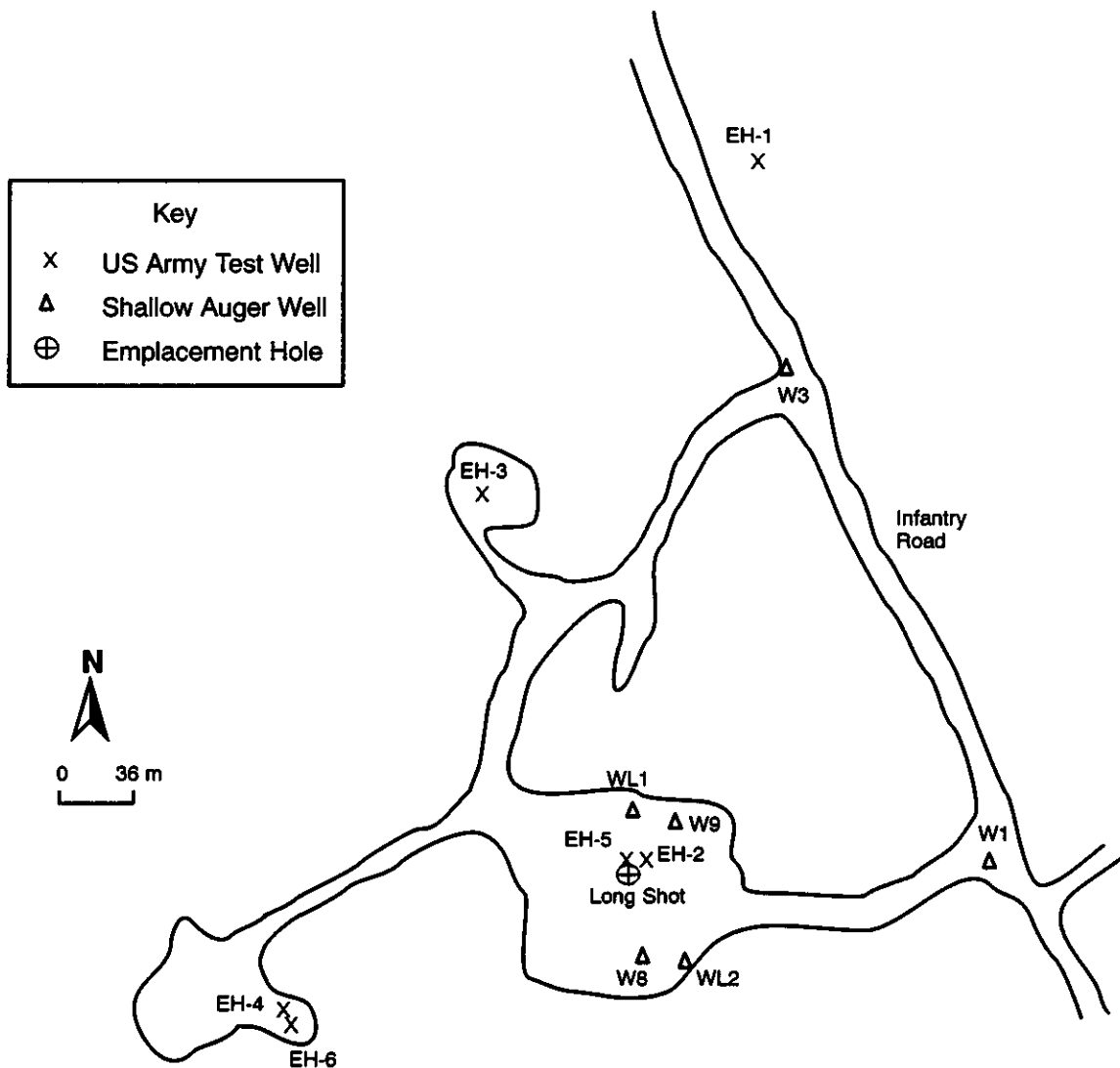


Figure 1.8. Location map showing wells and boreholes in the immediate vicinity of Long Shot. Modified from Fenix and Scisson, 1972.

(1978) estimated a slightly smaller cavity radius of 133 m, using a different approach. As with the other tests, the entire zone above the cavity to land surface is considered disrupted in the model. The collapse into the cavity void resulted in a very irregular subsidence of the land surface. The greatest subsidence, of about 12 m below pre-test elevation, occurs 400 m southeast of ground zero. Around it, the subsidence and associated faulting have left an enclosed basin that captured the White Alice Creek drainage and created a new lake, Cannikin Lake (Figure 1.10).

### 1.5 Geology of Amchitka Island

Amchitka Island is an exposure of the predominantly submarine Aleutian Ridge (Anderson, 1971). The Aleutian arc is comprised of the Aleutian Trench, extending from Kamchatka for 3,200 km east to the Gulf of Alaska, and a topographically high region adjacent to the north of the trench, the western two-thirds of which are known as the Aleutian Ridge. The Ridge is an almost completely

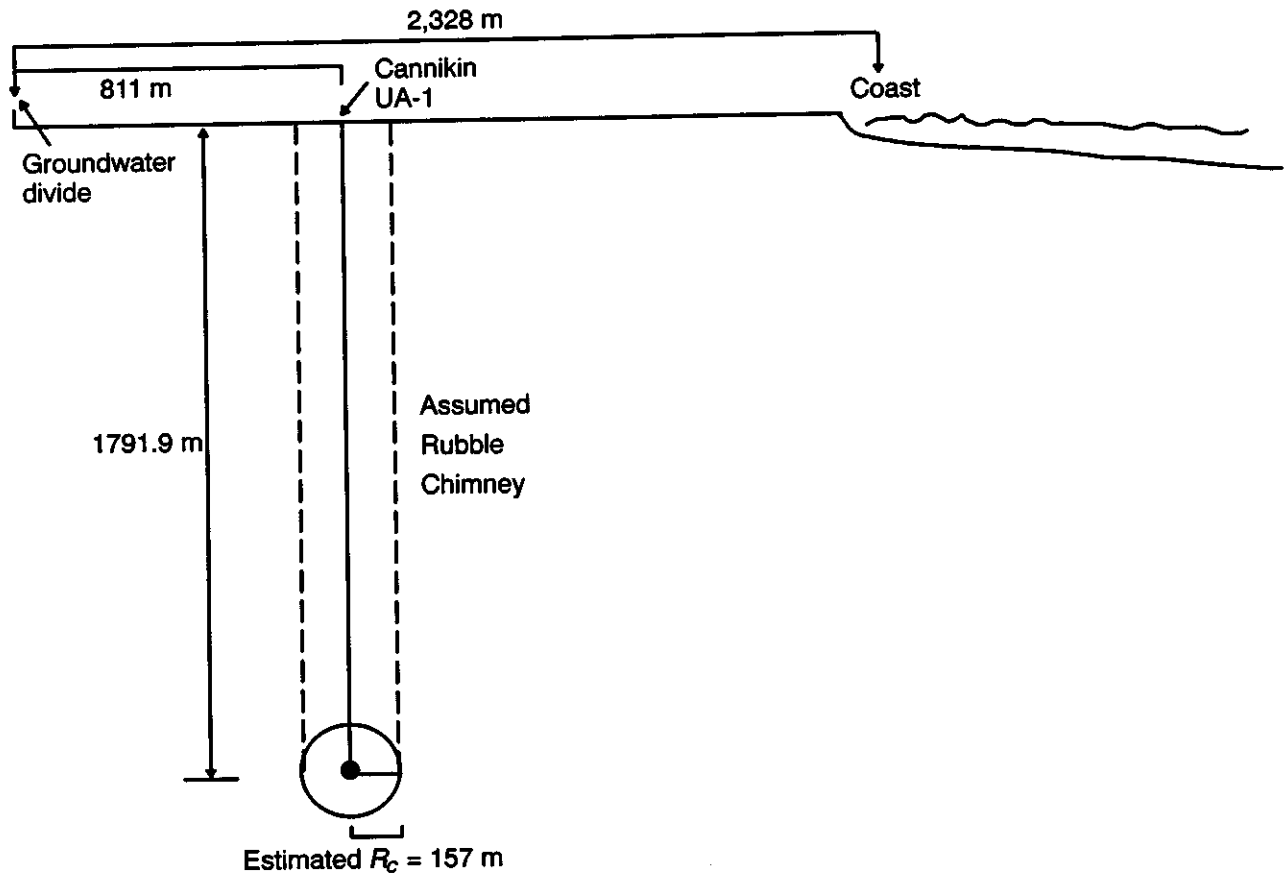


Figure 1.9. Schematic cross section of the Cannikin test and relevant features, scale approximate.

submerged mountain range that rises as much as 19,000 m above the ocean floor. The Aleutian arc, along with the Kuril and Kamchatka arcs, is the expression of the convergent plate boundary where the Pacific plate runs into the the Eurasian plate. The Aleutian Trench marks the subduction zone where the Pacific plate buckles downward, and the ridge is the crumpled and uplifted overriding continental plate. A prominent feature of the Ridge is the alignment of stratovolcanoes and composite cones, many of which remain active and define a narrow zone of active volcanism. Another characteristic of subduction zones is a concentration of great earthquakes, and the Aleutian arc is one of the world's most active earthquake belts. According to data collected prior to selection of Amchitka for higher-yield underground tests, at least 10 earthquakes of magnitude greater than 4.1 occurred within 100 km of Amchitka between March 1964 and March 1965 (U.S. AEC, 1967). Two of these were 7.5 in magnitude. Tsunamis commonly result from the earthquake activity, and in 1958, wave height reached 15 m.

### 1.5.1 Lithology/Depositional History of Amchitka Island

Amchitka Island primarily consists of Tertiary-age submarine and subaerially deposited clastic rocks of volcanic material, with lesser amounts of intrusive rocks. Four major stratigraphic units are recognized (Carr and Quinlivan, 1969), from oldest to youngest: 1) older breccias and hornfels, 2) pillow lavas and breccias of Kirilof Point, 3) Banjo Point Formation, and 4) the Chitka Point

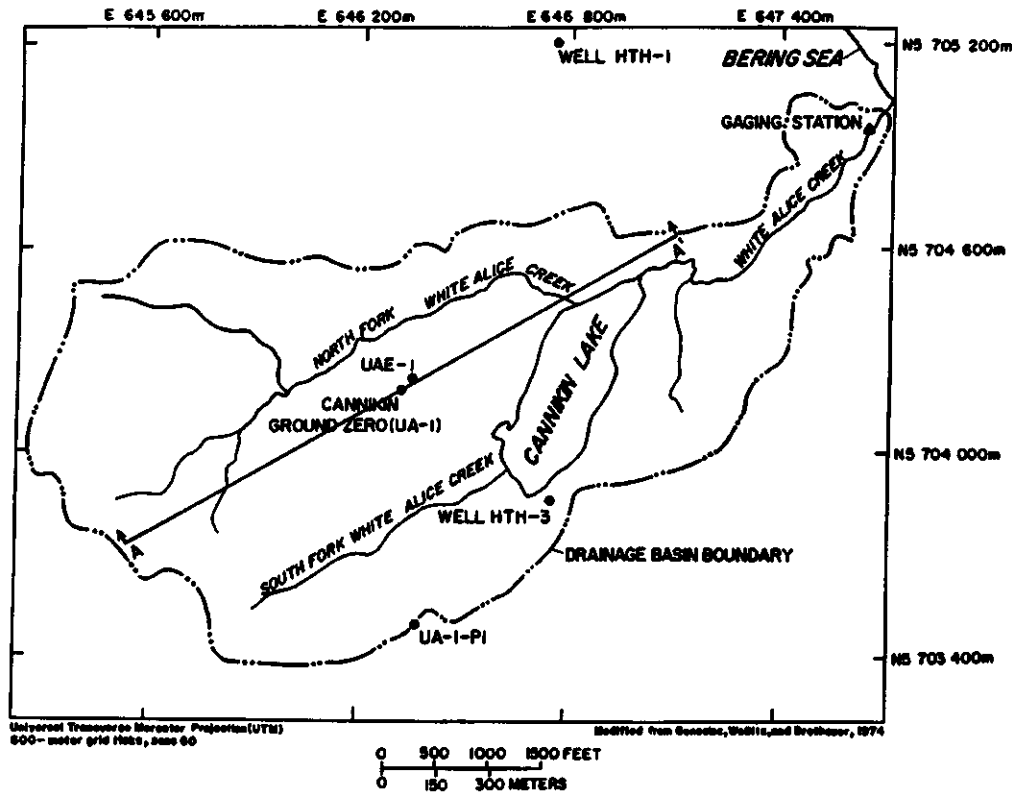


Figure 1.10. White Alice Creek drainage basin after the Cannikin test. From Claassen, 1978.

Formation. The older breccias and Kirilof Point units are sometimes reported as informal units of the Amchitka Formation (Lee and Gard, 1971). The lithology of the island is dominated by breccias and basalts. The following details are primarily from Carr and Quinlivan (1969).

The older breccias and hornfels of the Amchitka Formation, which are interbedded with sedimentary rocks, represent an early episode of submarine volcanic deposition. They are only exposed on the eastern end of the island (Figure 1.11). Lithologically, it consists of fine- to coarse-grained sedimentary breccias with 10 to 20 percent interbedded sandstone, siltstone, and claystone containing volcanic debris. Some alteration is present in the form of quartz, calcite and epidote. The working point for the Cannikin test was located in this unit, in an altered, locally autobrecciated pillow basalt, consisting of about half plagioclase feldspar, 25 percent chlorite, and 15 percent clinopyroxene, with minor calcite (Lee and Gard, 1971).

The pillow lavas and breccias of Kirilof Point are also only exposed on the eastern part of Amchitka and are also interpreted as being primarily of submarine deposition. Exposures reveal a partly glassy, generally monolithic breccia, with fragments generally less than a few centimeters in size. There are at least two pillow lava flows, and minor bedded sedimentary rocks. Rapid chilling is evident through vitric and devitrified glassy matrices, and glassy rinds around pillow structures, and vesiculated glass or pumice is also present. Where not glassy, the Kirilof breccias are yellowish to greenish due to alteration to palagonite, chlorite, nontronite, or green chalcedony. The Milrow working point was located in the pillow lavas and breccias of Kirilof Point (USGS, 1970).

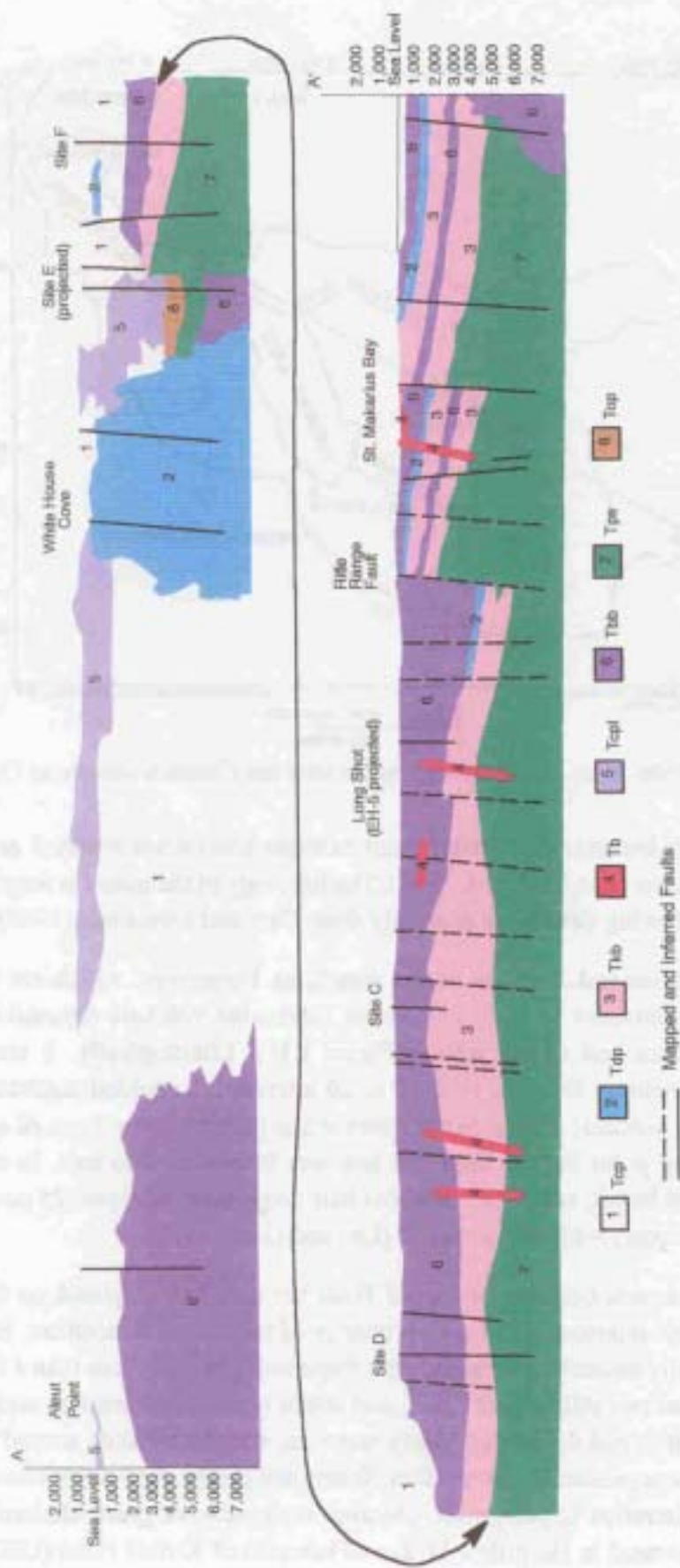


Figure 1.11. Geologic cross section along the long axis of Amchitka Island (after Carr *et al.*, 1971).

The Banjo Point Formation contains basaltic rocks of submarine deposition. It is a thick series of volcanic breccias, lapilli tuffs, and conglomerates with minor intercalated beds of volcanic sandstone, siltstone, shale, and tuff (U.S. Army Corps of Engineers and USGS, 1965). The volcanic breccias comprise the majority of the formation, and are poorly sorted, unstratified, and irregular in thickness. They are composed of angular basaltic or andesitic rock fragments set in a fine-grained matrix commonly containing fragments of pyroxene crystals. Some rocks contain considerable nontronite and montmorillonite. Marine shell fragments can be found, as well as thin beds of sediment, indicating deposition through submarine landslides and mudflows. Fragments of carbonized organic material, including logs, indicate a nearby landmass. The working point for the Long Shot test was located in the Banjo Point Formation (Nork *et al.*, 1965), in altered pyroclastic rocks of basaltic composition (Gard and Hale, 1964).

The Chitka Point Formation covers almost the entire northwestern half of Amchitka Island and consists almost entirely of subaerially deposited hornblende andesite volcanic rocks (Carr and Quinlivan, 1969). The lower part of the formation consists of varicolored heterogeneous breccia consisting of fragments of hornblende andesite in a tuffaceous matrix, conglomerate with andesite cobbles, a few hornblende andesite lava flows (some with large green pyroxene crystals), and minor sedimentary layers. Much of the Chitka Point Formation has been altered by hydrothermal activity. Weakly altered zones consist of chloritic minerals and pyrite, while the rock in more intensely altered zones is converted to masses of silica, clay zones, iron oxides, pyrite, and chlorite minerals.

A variety of intrusive igneous rocks is present on Amchitka, exposed as dikes and sills, and more voluminous complexes of diorites and andesites. They are exposed on the east and west parts of the island, and strong propylitic alteration and silicification of rocks in the mountainous part of the island suggest the proximity of a large intrusive mass (Carr *et al.*, 1969). Dikes range from olivine-bearing basalts to hornblende and pyroxene andesite to quartz diorite. Quaternary deposits are unconsolidated sands and gravels in fault depressions, beach deposits, and stabilized dunes. Much of the land surface on the southeastern half of the island is covered by a mantle of maritime tundra and peat.

In the part of the island where the nuclear tests were conducted, the stratigraphic section is generally dipping southeastward (Carr and Quinlivan, 1969). Drilling and mapping associated with Long Shot indicated that the Banjo Point Formation strikes N55°E and dips from 10° to 15° to the southeast (Gard and Hale, 1964).

### 1.5.2 Lithology Specific to the Testing Areas

Six areas were evaluated on Amchitka for the STS program, denoted by the letters A through F (Figure 1.4). Sites B and C became Milrow and Cannikin, respectively, and Long Shot is located between them. The preference for sites B and C was largely based on the predictability of the subsurface geology at those sites, due to extrapolations from Long Shot borehole data (U.S. AEC, 1967). In other words, the three tests were sited so that they would encounter similar geologic units. They are discussed below in order from southeast to northwest.

Subsurface data from the Milrow site come primarily from the exploratory borehole UAe-2 (Figure 1.12). This well was located at UTM coordinates of N 5,698,166.48 m, E 651,716.53 m,

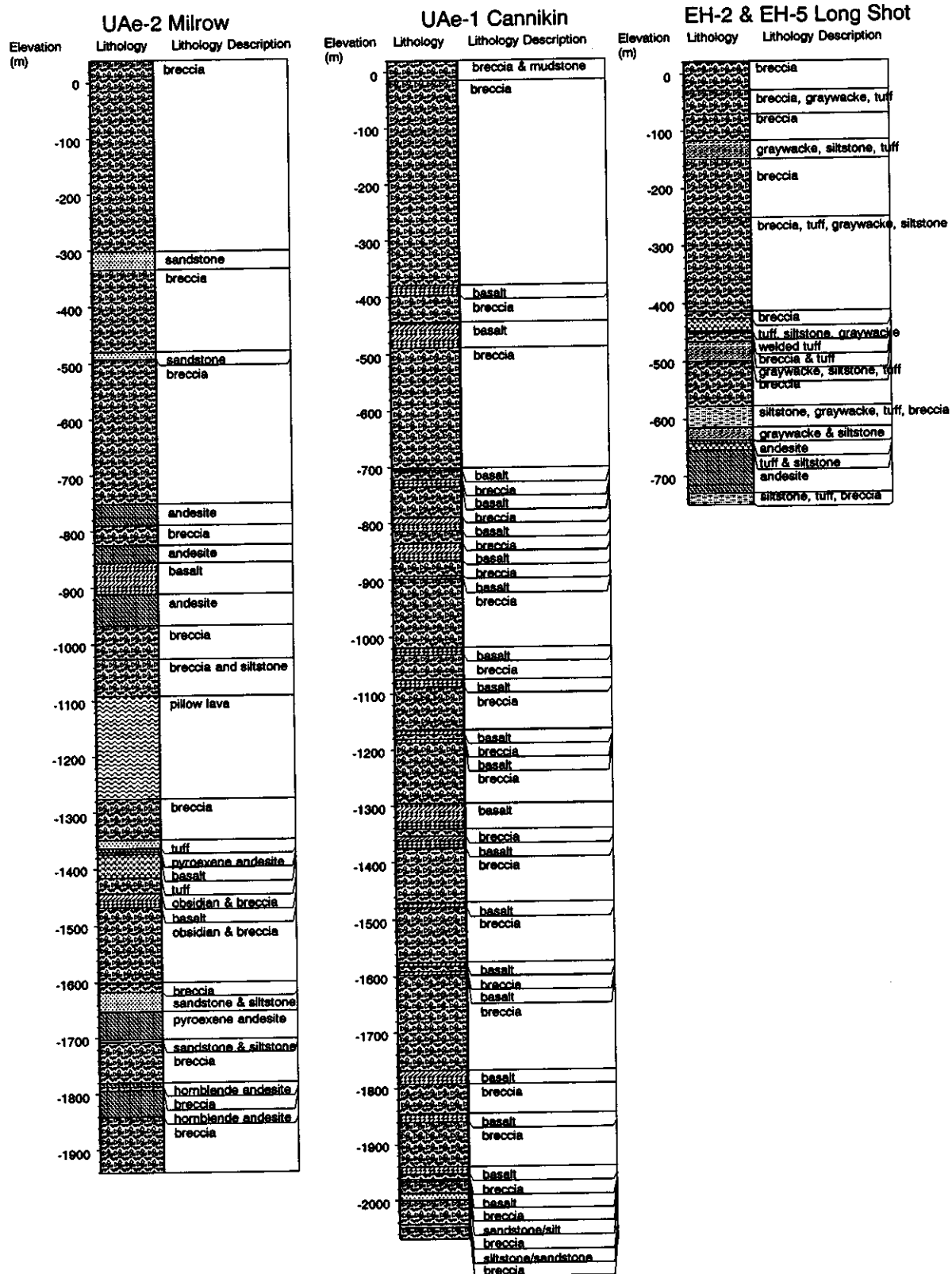


Figure 1.12. Construction diagram, lithologic log and summary of hydraulic tests, holes UAc-2, UAc-1, EH-2 and EH-5, Amchitka Island, Alaska. From Ballance, 1973a,b.

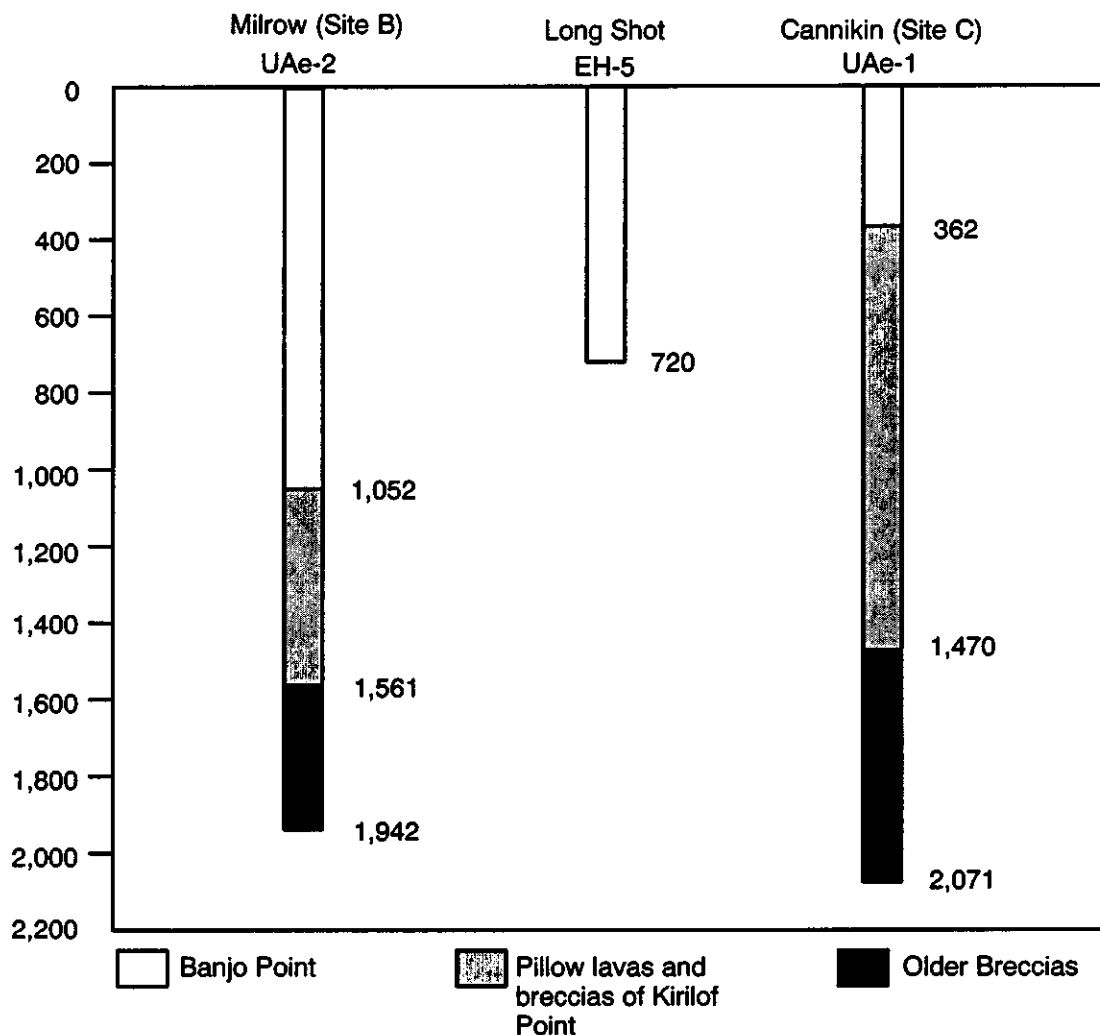


Figure 1.13. Stratigraphic section encountered in the exploratory boreholes for the three test sites (numbers are elevation below sea level).

zone 60, with a ground elevation of 39.47 m. The hole was drilled to 1,981.2 m. The borehole penetrated the Banjo Point Formation from land surface to a depth of 1,091 m, the pillow lavas and breccias of Kirilof Point from 1,091 to 1,600 m, and bottomed in the Older Breccias (encountered from 1,600 to the total depth of 1,981 m (Figure 1.13, note the figure expresses elevation not depth). The actual working point in borehole UA-2 (the device emplacement hole) was in the pillow lavas and breccias of Kirilof Point. Most of the rock penetrated by UAe-2 is volcanic breccia, andesite, and basalt. Fenske (1972) estimated the geologic section at UAe-2 to be comprised of 60 percent breccia and 32 percent basalt. Lithologic information is detailed by Snyder (1968a), while physical properties of core samples (*e.g.*, porosity and bulk density) are given by Lee (1969a).

Boreholes drilled during Long Shot investigations were contained within the Banjo Point Formation. Volcanic breccia was the primary lithology encountered, with some tuff, sandstone and siltstone containing volcanic rock fragments (Figure 1.12). Two andesite sills were also encountered near the bottom of the boreholes. Boreholes EH-3, -5, and -6 have surface locations within 180

m of each other and are angled so as to intersect at depths of about 610 m. Despite this proximity, correlations can only be made in very general terms until the holes are within 30 m or less of each other. No satisfactory correlations were made with borehole EH-1, located at a distance of about 300 m from the other holes. Detailed lithologic data and physical property data for Long Shot boreholes can be found in U.S. Army Corps of Engineers and USGS (1965).

The stratigraphic section at Cannikin was investigated in the UAe-1 exploratory borehole (Figure 1.12). This well is at UTM coordinates N 5,704,210 m, E 646,350 m, with a ground elevation of 62.79 m. From land surface to 425 m, the borehole penetrates the breccias, siltstones, and sandstones of the Banjo Point Formation (Lee and Morris, 1968). Glassy breccias and pillow lavas of Kirilof Point were encountered from 425 to 1,533 m below land surface. Propylitized breccias, basaltic siltstone and sandstones, andesites and basalts, all of the Older Breccias Formation, occur from 1,533 m to the 2,134 m total depth of the hole (Figure 1.13, expressed in elevation). The test chamber in the Cannikin emplacement hole, UC-1, was completed from 1,783 to 1,799 m in a zeolitic basalt.

### 1.5.3 General Structure of Amchitka Island

There are contradictory interpretations of the regional stress field around Amchitka. Based on the general structural setting of the Aleutian arc, as well as data from Long Shot, McKeown *et al.* (1967) indicate that the region around Amchitka Island is currently under compression. The arc itself represents the collision of continental and oceanic plates. While acknowledging the crustal foreshortening occurring across the Aleutian arc, Anderson (1971) interprets the geology of Amchitka and regional tectonic features, inferred largely from geophysical data, as providing little evidence for compression. Instead, he suggests that the principal deformation resulted from tensional stress brought on by a rising and spreading core of intrusive igneous rock overlain by a relatively brittle envelope.

There are strongly developed joint and fault systems on the island, indicated by prominent linear topographic features. Near the Long Shot site, the dominant trend of the lineations is N55°E to N60°E, corresponding to the strike of bedding in the area (U.S. Army Corps of Engineers and USGS, 1965). Later work (Carr *et al.*, 1969) concluded that faults are not as abundant as lineaments suggest in the central part of the island, but that the lineaments tend to reflect joints and lithologic contacts, accentuated by erosion.

Approximately a dozen major fault zones were identified in the central part of the island (where the three underground nuclear tests were conducted), a few of which may have a width of up to 1,000 m, and within which the rocks may be highly fractured. Nearly all of these major faults trend about N70°E, though there is a second direction of structural weakness bearing northwest. The major fault dip is steeply to the northwest at 75°-90°. Vertical displacements of at least 300 m are noted and indications are that the most recent fault movement had a strong lateral component. It is suspected that at least the larger faults are strike-slip.

### 1.5.4 Structure Specific to the Testing Areas

The underground test locations were sited so as to avoid known fault zones (U.S. AEC, 1967). As a result, all three tests are located approximately midway in structural blocks between known or suspected faults (Figure 1.14).

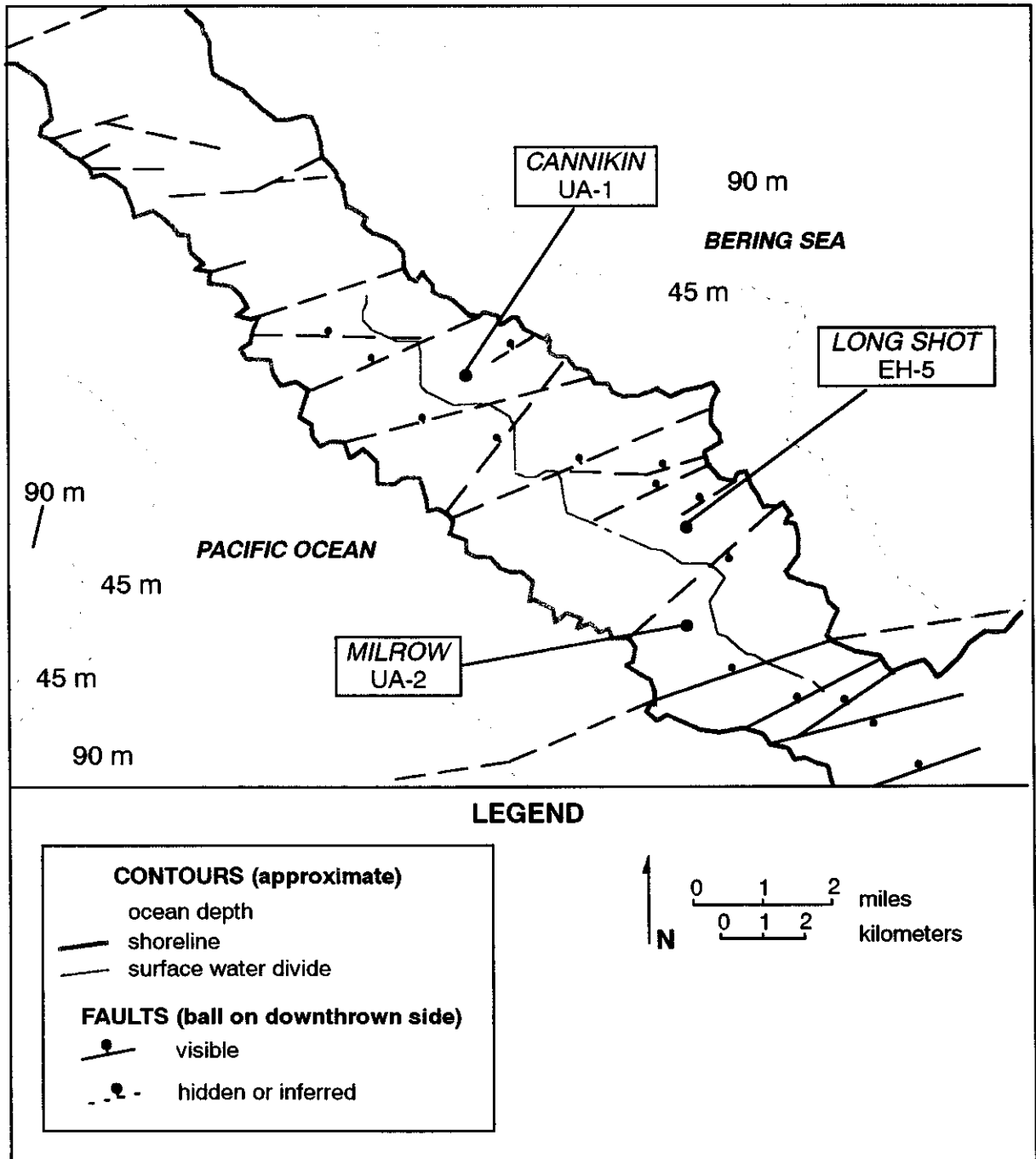


Figure 1.14. Schematic map of underground testing areas showing major features and bathymetry (after von Huene *et al.*, 1971).

Structurally, Milrow is located in a block between two faults. Milrow is about 1,200 m north of the Rifle Range Fault. This fault trends N70°E, has a stratigraphic displacement of 1,220 m, and is thought to be represented by a fracture zone as much as 300 m wide (Morris and Gard, 1970). The Rifle Range Fault is believed to dip steeply northwest (Carr *et al.*, 1969). Another fault is inferred about 1,000 m north of Milrow (McKeown *et al.*, 1970), trending about N50°E.

Long Shot is bounded on the northwest and southeast by two strong lineaments, believed to be faults striking N55°E (Gard and Hale, 1964; McKeown *et al.*, 1967). Though topography suggests the intervening 610-m-wide block is a graben, McKeown *et al.* (1967) suggest Long Shot is located in a horst. Drillhole EH-1 was located on the bounding fault to the northwest (as indicated by seismic evidence); the hole had to be abandoned at a depth of 490 m due to lost circulation. During drilling of EH-3, a significant fault was encountered at a depth of 611 m. It was characterized by rock and clay gouge about one meter wide. Most fractures encountered in cores are hairline, with slickensides, and many are cemented by calcium carbonate and zeolites. Several open fractures were encountered in EH-1, one of which had a 1-cm-thick coating of botryoidal calcium carbonate (Gard and Hale, 1964).

Two major northeast-trending faults bound the Cannikin test area (Carr and Quinlivan, 1969). The Teal Creek fault occurs 1,070 m northwest of Cannikin, and an unnamed fault occurs 760 m south. The Teal Creek Fault strikes approximately N65°E and dips 80° to the northwest (Gard, 1971). The unnamed fault strikes about N75°E with an unknown dip. A much smaller fault is shown as inferred on a geologic map of the Cannikin area by Gard (1971) and is mapped from the Bering coastline, running about 610 m in the general direction of the emplacement hole.

## 1.6 Hydrogeology

The hydrogeology beneath the surface at Amchitka is governed by the dynamics of the saltwater intrusion system typical of islands. The groundwater system consists of a freshwater lens floating on seawater. To sustain this lens, there must be active groundwater circulation. Rainfall that infiltrates is fresher, and less dense, than the underlying seawater. Continued recharge results in the buildup of a lens of freshwater floating above the seawater, and the flow of freshwater from the center of the island outward to the ocean. This is analogous to an iceberg in that the majority of the freshwater lens, including the seepage face where discharge occurs, is below sea level. Under non-stressed conditions, such as occur on Amchitka (no pumping of groundwater), a steady-state condition is reached where recharge from rainfall is balanced by discharge along the seepage face to the ocean. The thickness of the freshwater lens is controlled by the hydraulic conductivity of the aquifer, the recharge flux, the land elevation, dispersion and anisotropy in hydraulic conductivity.

Groundwater flow is generally characterized by recharge along the water table, downward flow in the interior of the island, and upward flow approaching the coast, with freshwater discharge seeps along the seafloor (Figure 1.15). The lateral component of the hydraulic gradient is from the axis of the island to the coasts on either side, though vertical components of flow are important. Although at much lower flux rates than occur in the freshwater lens, there is a cycle of saltwater flow beneath the island as well. The saltwater flow is caused by the diffusion of salt into the overlying freshwater lens in the transition zone. The salt removed by this process is replenished by recharge

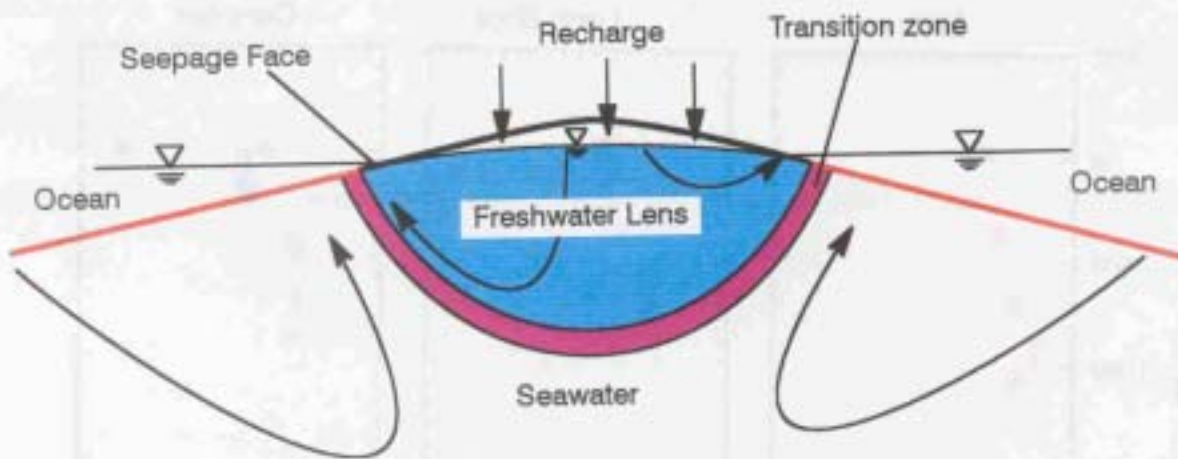


Figure 1.15. Saltwater intrusion beneath island aquifers. Typical flowpaths are indicated by the curved arrows.

of the saline groundwater system through the seafloor at distances greater than the zone of freshwater discharge.

Exclusive of the higher altitude area to the northwest, the water table at Amchitka is very near to land surface. Shallow wells drilled in the testing areas encountered groundwater at depths of essentially zero to several meters below land surface (Essington *et al.*, 1971). Significant runoff of rainfall to ponds and streams occurs (Gonzalez, 1977), consistent with nearly saturated subsurface conditions. Dudley *et al.* (1977) observed that most precipitation runs off in stream channels.

Hydraulic head measurements with depth (Figure 1.16 and Figure 1.17) demonstrate decreasing head values with increasing depth (Ballance, 1968), consistent with the downward flow expected in the island center. Head data are discussed in more detail in the section on flow parameters (Section 2). Though the hydraulic gradient supports the oceanward movement of groundwater, Dudley *et al.* (1977) conclude that the hydraulic conductivity in the upper few hundred meters is not high enough for large rates of flow, leading to most groundwater beneath Amchitka moving in very local systems to discharge in lakes and streams.

Lithologic descriptions, the rock physical properties, and geophysical logs indicate that the aquifers on the island occur in fractured rock units (Fenske, 1972) and, generally, most investigators have applied a conceptual model of predominantly fracture flow between matrix blocks of relatively high porosity. By analyzing water level fluctuations in wells as compared to barometric and tidal fluctuations, Fenske (1972) identified two, interconnected components to the Amchitka flow system: 1) a system of high porosity and extremely low hydraulic conductivity, and 2) a system with low porosity and relatively high hydraulic conductivity. Dudley *et al.* (1977) conclude that hydraulic testing strongly indicates that fractures are the primary avenues of fluid movement. They note that fractures tend to close under greater lithostatic load, implying decreasing hydraulic conductivity

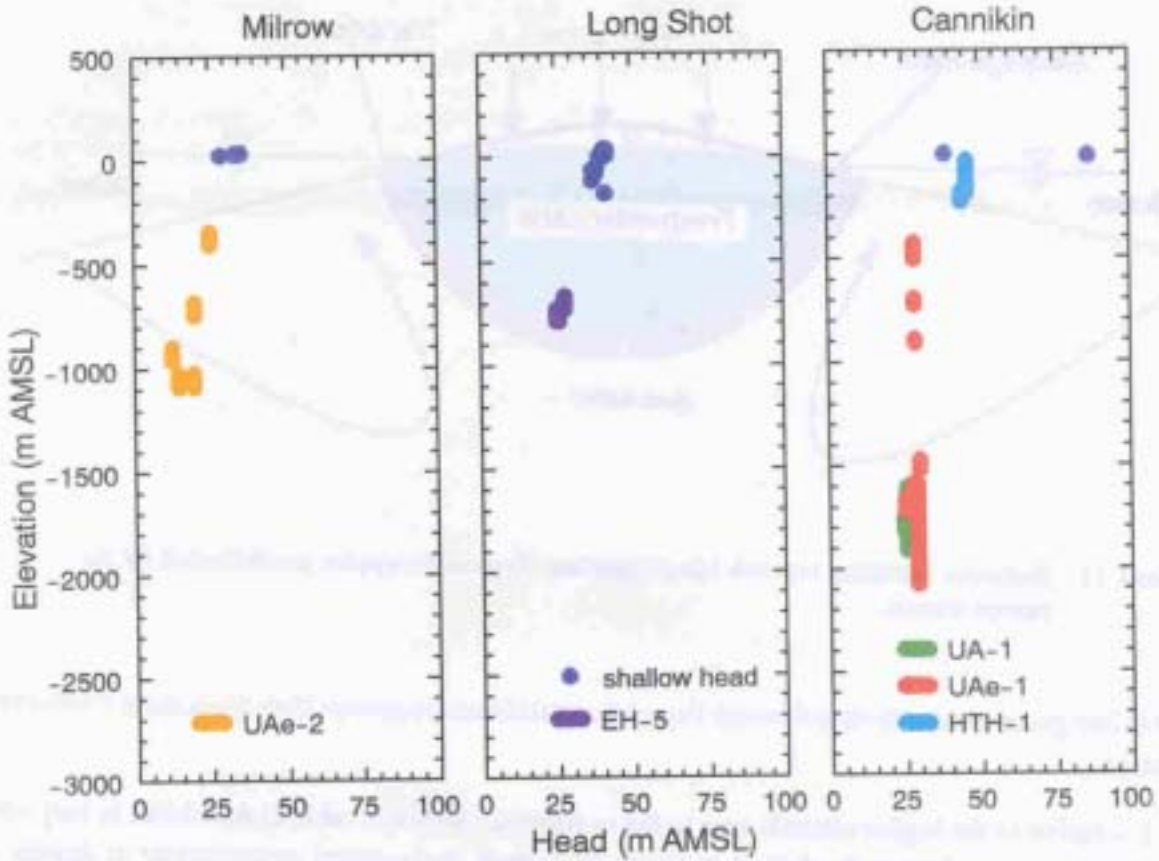


Figure 1.16. Head measurements at different wells as a function of elevation.

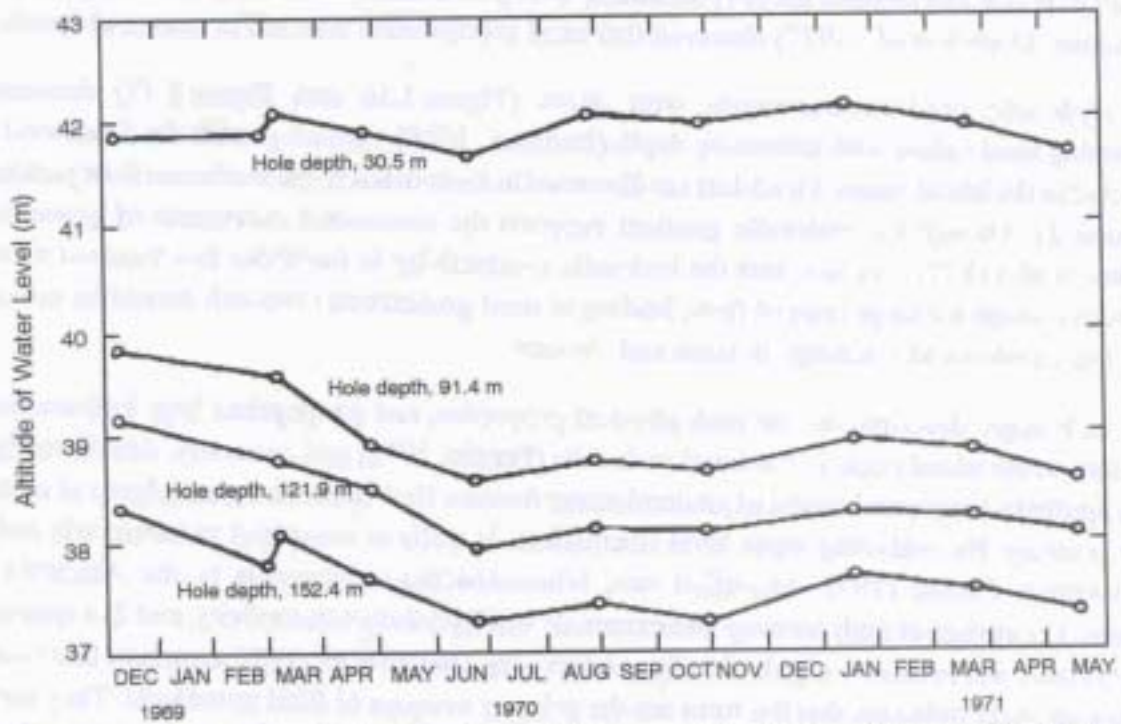


Figure 1.17 Water levels in shallow boreholes at the Long Shot site. From Dudley *et al.* (1977).

with depth. The development of zeolites and chlorites in fractures from the alteration of the volcanic rocks further reduces the hydraulic conductivity (Dudley *et al.*, 1977).

The depth of the transition from freshwater to seawater is an important feature in island hydraulic systems, as groundwater velocities are much higher above this transition zone than below it. Based on hydraulic head profiles for the three sites, Fenske (1972) estimated the bottom of the freshwater lens to be 780 m below sea level at Milrow and about 1120 m below sea level at Long Shot and Cannikin. Fenske (1972) notes that the results indicate an asymmetry of the freshwater lens. Fenske compared the hydraulic head analysis with the chemical analyses of water samples and found good agreement for Milrow. The relatively shallow depth of the testing at Long Shot did not allow sampling or measurements in the transition zone nor underlying seawater zone. The chemical composition of groundwater samples from the boreholes at Cannikin reveals a much less saline water with depth than encountered at Milrow (as discussed in the following section). After evaluating the drilling methods and hole histories for UAe-1, UAe-2, and UAe-6h, Fenske (1972) concluded that the total dissolved solids content of about one-tenth of the concentration expected below the predicted interface was probably due to injection of drilling fluid during the long and difficult hole construction in UAe-1. Dudley *et al.* (1977), however, conclude that the data are substantially correct and indicate a freshwater lens extending to an altitude of at least -1,700 m, based on generally corroborating data from the emplacement hole, UA-1.

### 1.7 Hydrochemistry

Consistent with the island hydraulic system described above, the profile of groundwater salinity with depth beneath an island is expected to reflect low salinity at shallow depths and a salinity consistent with seawater beneath the freshwater lens. The contact between freshwater and seawater cannot be sharp due to mixing caused by diffusion driven by the chemical gradient, and by dispersion caused by hydrogeologic heterogeneity, short-term head fluctuations (*e.g.*, tidal effects), and long-term sea-level changes.

Chemical data for water samples from the island are reported by Beetem *et al.* (1971), as are their sample collection and analytical procedures. Charge balance checks of their analyses are all less than five percent off balance, with the vast majority being within two percent. Groundwater samples from wells at Long Shot were analyzed and reported by the U.S. Army Corps of Engineers and USGS (1965), though many of their analyses were incomplete in that they did not include all major anions and cations. Selected analyses from these sources are presented in Table 1.2.

The dissolved solids content of seawater collected off Amchitka is reported as 34,700 mg/L for the Bering Sea and 34,800 mg/L for the Pacific Ocean (Beetem *et al.*, 1971). Samples of surface water were collected from lakes and streams on the island and have a mean total dissolved solids (TDS) content of 145 mg/L and 137 mg/L, respectively (from residue on evaporation, Beetem *et al.*, 1971). Water from springs is similar, with a TDS of 143 mg/L. These relatively high salinities for surface water reflect the influence of the near-coast environment and salt spray. Though Na dominates the cations, Ca and Mg are present in proportions generally similar to seawater (Figure 1.18).

Groundwater samples from boreholes on Amchitka have primarily been collected by swabbing discrete intervals, though a few pumped samples from large intervals have also been collected.

Table 1.2. Representative groundwater chemistry data from the three testing areas (from Ballance *et al.*, 1971, and U.S. Army Corps of Engineers and USGS, 1965).

Zone Sampled (m)	Date	SiO <sub>2</sub>	Al	Fe	Mn	Mg	Ca	Sr	Li	Na	K	HCO <sub>3</sub>	CO <sub>3</sub>	SO <sub>4</sub>	Cl	F	NO <sub>3</sub>	PO <sub>4</sub>	TDS residue	EC	pH
UAe-2 water analyses (Milflow).																					
379.8 - 440.1	11/16/1967	15	-	0.01	0.75	0.1	260	2.2	0.2	1,980	20	106	0	890	3000	0.6	1.1	0.9	6,390	9,740	7.8
719.3 - 779.7	11/16/1967	13	-	0.01	0.75	0.1	970	7	0.2	4,800	60	380	0	1,000	8100	0.4	0.5	0.3	15,600	21,900	7.4
822.4 - 882.7	11/16/1967	17	-	0.01	2.6	0.1	1,380	11	0.2	6,800	70	360	0	1,800	11,900	0.7	0.1	0.4	22,300	30,400	7
873.6 - 933.9	11/17/1967	15	-	0.01	2.3	0.1	1,470	10	0.2	7,500	68	340	0	2,000	12,000	0.5	0.1	0.3	23,200	29,900	7.5
933.9 - 994.3	11/17/1967	8	-	0.01	2.6	0.1	1,450	12	0.2	6,800	55	360	0	1,800	11,900	0.6	0.1	0.5	23,100	30,700	7.7
1057.6 - 1127.8	11/17/1967	19	-	0.01	3.5	0.1	1,560	12	0.2	7,100	70	400	0	2,000	11,900	1	0.1	0.3	24,200	32,800	7.3
1169.8 - 1230.2	12/20/1967	3.1	-	-	3	140	1,800	20	0.5	8,200	90	36	0	1,600	15,000	0.1	5.4	0.1	29,400	41,000	6.9
1466.7 - 1527	12/20/1967	30	-	-	3.4	160	1,900	21	0.5	8,700	100	42	0	1,600	16,000	0.1	4	0.1	31,600	41,000	6.9
1530.1 - 1590.4	12/21/1967	34	-	-	3.4	170	1,900	20	0.5	8,400	120	43	0	1,800	16,000	0.1	0.2	0.1	30,600	41,500	6.9
EH-5 water analyses (Long Shot).																					
390 - 451	11/06/1964	-	-	-	-	-	-	-	-	-	-	341.6	0	-	65	-	-	-	-	-	8.35
390 - 451	11/06/1964	-	-	-	-	-	-	-	-	-	-	305	0	-	71	-	-	-	-	-	8.35
602 - 663	11/05/1964	-	-	-	-	-	-	-	-	-	-	402.6	0	-	337	-	-	-	-	-	8.0
662.9 - 723.9	11/03/1964	16	0.12	0	0	1.5	8.6	0	0	512	5.4	330	14	355	351	2.7	0.1	0.00	1460	2360	9.4
663 - 724	11/03/1964	-	-	1.5	0.3	5	30	-	-	-	-	257.2	0	400	334	-	0.5	-	-	-	8.25
723.9 - 784.6	11/03/1964	5.2	0.17	0	0	1.7	7.7	0	0	572	6.9	332	18	410	417	1.8	0.2	0.01	1650	2690	9.4
724 - 785	11/03/1964	-	-	1.05	0	30	20	-	-	-	-	207.4	60	380	405	-	0	-	-	-	8.2
EE Hole																					
45.7 - 50.3	09/16/1967	20	-	0.54	0.01	1.4	6.8	-	-	130	5.1	184	16	28	76	0.2	1.6	-	-	627	8.9
121.5 - 126.5	09/19/1967	27	-	0.65	0.01	0.6	19	-	-	520	8.9	42	61	363	500	0.6	2.0	-	-	-	9.9
UAe-1 water analyses (Camikin).																					
487.3 - 564	09/29/1967	13	-	-	<0.1	0.9	120	1.5	0.1	420	6.0	0	3	110	620	1.7	0.5	-	-	3,190	11.8
759.2 - 786.6	09/28/1967	28	-	-	<0.1	1.2	53	0.7	0.1	310	5.0	0	39	150	520	2.3	0.4	-	-	2,190	11.0
951.2 - 969.5	09/28/1967	21	-	0.4	<0.1	1.7	68	0.8	0.1	530	5.0	0	37	220	690	2.2	0.4	0.1	1,640	2,560	10.3
1,356.7 - 1,387.2	09/29/1967	13	-	<0.1	<0.1	4.1	400	4.1	0.1	1,000	10	0	3	250	2,000	1.3	0.1	<0.1	3,740	6,530	11.6
1,643.9 - 1,655.5	08/13/1967	15	-	<0.1	0.03	0.3	293	3.2	0.2	1,080	10	21	48	320	1,850	0.8	0.2	0.1	3,920	6,340	10.0
1,646.3 - 1,725.0	08/11/1967	20	-	<0.1	0.06	1.5	278	3.1	0.2	1,100	7.9	32	12	320	1,860	0.8	0.5	0.1	3,980	6,430	8.7
1,646.3 - 1,725.0	08/11/1967	16	-	<0.1	<0.1	3.7	14	0.5	0.1	400	9.0	243	0	97	432	0.2	0.4	0.3	1,100	1,900	8.2
1,724.4 - 1,784.8	08/11/1967	22	-	<0.1	<0.1	0.2	289	3.2	<1	1,200	7.0	18	15	330	2,060	1.9	0.4	0.1	4,310	6,710	8.9
1,786.0 - 1,826.2	08/11/1967	21	-	<0.1	0.04	1.6	268	3.0	0.2	1,140	7.9	19	11	310	2,040	0.6	0.6	<0.1	4,220	6,350	8.7
1,802.4 - 1,862.2	08/28/1967	15	-	0.02	0.01	1.0	170	1.8	0.1	730	5.0	30	4	210	1,190	1.4	0.4	0.1	2,690	4,270	8.6
1,802.4 - 1,862.2	08/28/1967	18	-	<0.1	0.08	0.8	164	2.2	0.2	760	6.8	32	0	224	1,260	0.6	0.3	0.1	2,540	4,270	7.8
1,850.6 - 1,911.0	08/27/1967	15	-	0.13	<0.1	5.2	280	2.5	0.1	940	7.0	0	14	290	1,740	1.8	0.2	0.1	3,580	5,970	10.3
1,850.6 - 1,911.0	08/27/1967	14	-	<0.1	0.03	0.3	290	3.3	1.3	1,020	7.9	24	41	275	1,770	0.6	0.1	<0.1	3,680	6,000	9.8
UA-1 Sump																					
1525+	11/19/70	28	-	-	-	0.1	220	2	0.1	1,100	8.2	0	23	280	1,900	2.5	0.1	-	-	5,900	9

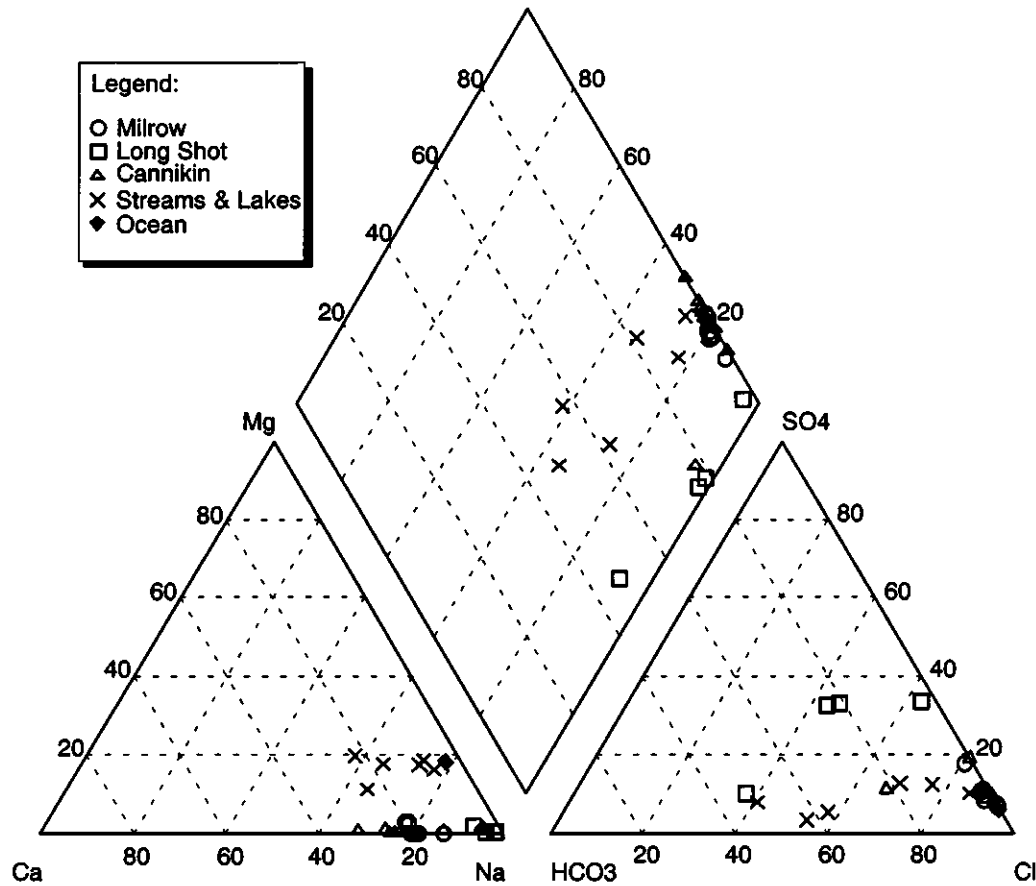


Figure 1.18. Relative ion percentages for water samples from Amchitka.

Collection of samples representative of formation water can be difficult due to the need to purge drilling fluids. High pH values are reported for some of the groundwater samples, indicating they were affected by contact with cement during grouting operations. The problem of groundwater sample representativeness is discussed further in section 2, regarding model parameter uncertainty.

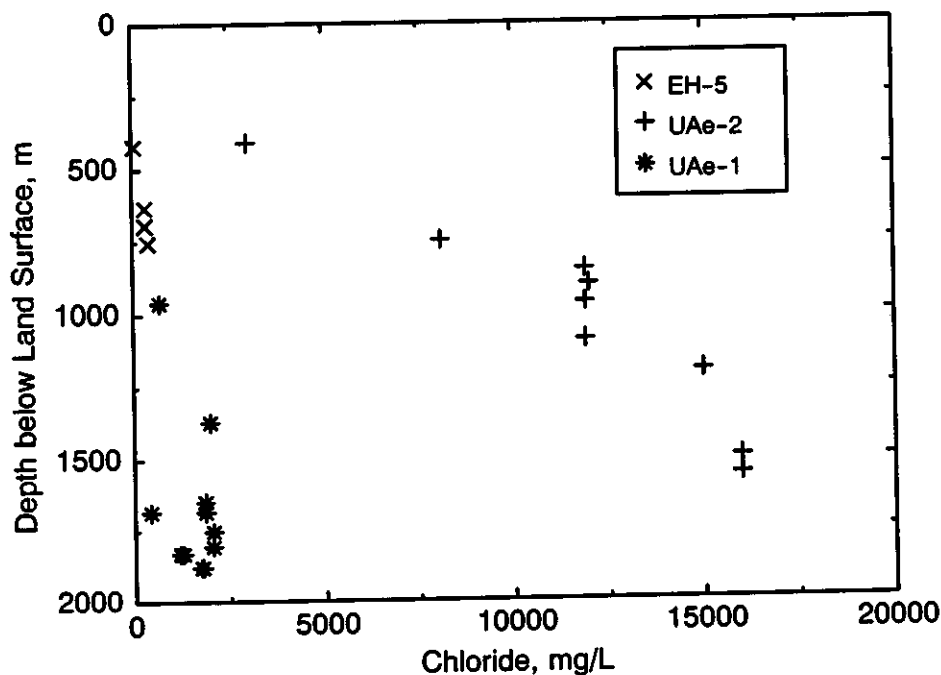
In terms of major ion percentages, the groundwater at Amchitka is distinguished from the surface water and seawater by the relative absence of Mg. Concentrations of Ca and  $\text{HCO}_3$  are highly variable, some of which may be due to cement contamination as indicated by very high pH values for certain samples. The Long Shot groundwater analyses are atypical of the other groundwater, having a higher proportion of Na,  $\text{HCO}_3$ , and  $\text{SO}_4$ . The Long Shot holes were drilled with a bentonite mud that was impossible to purge from the holes without collapse, so these chemical differences may reflect residual drilling fluids. One of the Cannikin samples displays a similar chemical character, and the pH values for all of the Cannikin and Long Shot samples are considerably higher than those measured for the surface water and at Milrow.

The groundwater freshwater lens and underlying saltwater can be identified by samples collected by swabbing packer-isolated zones in well UAe-2. These zones are typically about 60 m in length and thus the samples represent composites of borehole fluid through that length. The chemical analysis of

these samples (Table 1.2; Beetem *et al.*, 1971) clearly defines the increase in salinity with depth to near-seawater concentrations. At Long Shot, electrical conductivity measurements led workers to identify “saltwater encroachment” in deeper groundwater samples, but salinities close to seawater were not found in chemical analysis. Groundwater from 670 to 793 m below land surface at Long Shot contained 350 to 415 ppm chloride and TDS contents of 1460 to 1650 mg/L (U.S. Army Corps of Engineers and USGS, 1965). Water samples from borehole UAe-1 at the Cannikin site show little relationship between salinity and depth. This scatter has been argued as evidence of drilling fluid contamination by Fenske (1972), though Dudley *et al.* (1977) argue that the similarity in salinity for sump samples collected during mining the Cannikin cavity is evidence of the samples being representative of groundwater.

Using chloride as a conservative-ion indicator of salinity, the transition zone midpoint can be defined as the depth where the groundwater has a chloride content midway between the surface water value and the seawater value (*i.e.*, 9,025 mg/L, halfway between about 50 and 18,100 mg/L Cl). At Milrow, that occurs at an elevation of about 850 m below sea level (Figure 1.19), and at the other two sites, that salinity is not achieved in water from the sampled intervals.

Four carbon-14 age dates have been reported for Amchitka groundwater (Table 1.3). Two samples from UA-1-HTH-1, seaward of Cannikin, were analyzed for carbon-14. The interval from 183.5 to 234.7 m gave an apparent age (uncorrected for non-radiogenic carbon, an error expected to be small in a volcanic aquifer) of 8,410 years; the interval from 227.4 to 278.6 m had an apparent age of 17,880 years (Ballance and Dinwiddie, 1972). A sample from the interval of 679.8 to 740.1 m below sea level in UAe-2 gave an apparent age of 5,260 years (Fenske, 1972). A deeper sample, from



888.3 to 906.2 m below sea level, collected from UAe-1, had an apparent age of 11,000 years (Fenske, 1972). Though no consistent trend in age with depth can be discerned from one well location to another, the large increase in age across the 100-m interval in HTH-1 was considered real by Ballance and Dinwiddie (1972). The implication of the carbon-14 data is that even in the shallower, freshwater portion of the island hydraulic system, groundwater residence times are long and overall velocity is low.

Table 1.3 Carbon-14 data for Amchitka groundwater samples. From Fenske (1972) and Ballance and Dinwiddie (1972).

Well	Depth Interval, m	Conductivity, $\mu\text{mhos/cm}$	Uncorrected C-14 age, yrs
HTH-1	183.5-234.7	590	8410
HTH-1	227.4-278.6	800	17,880
UAe-2	679.8-740.1	~20,000*	5260
UAe-1	888.3-906.2	~2400*	11,000

\*estimate based on sample from nearest depth interval reported by Beetem *et al.* (1971)

**THIS PAGE LEFT INTENTIONALLY BLANK**